

Bayesian Reinforcement Learning for Automatic Voltage Control under Cyber-Induced Uncertainty

Abhijeet Sahu, *Student Member, IEEE*, and Katherine Davis, *Senior Member, IEEE*

Abstract—Voltage control is crucial to large-scale power system reliable operation, as timely reactive power support can help prevent widespread outages. However, there is currently no built in mechanism for power systems to ensure that the voltage control objective to maintain reliable operation will survive or sustain the uncertainty caused under adversary presence. Hence, this work introduces a Bayesian Reinforcement Learning (BRL) approach for power system control problems, with focus on sustained voltage control under uncertainty in a cyber-adversarial environment. This work proposes a data-driven BRL-based approach for automatic voltage control by formulating and solving a Partially-Observable Markov Decision Problem (POMDP), where the states are partially observable due to cyber intrusions. The techniques are evaluated on the WSCC and IEEE 14 bus systems. Additionally, BRL techniques assist in automatically finding a threshold for exploration and exploitation in various RL techniques.

Index Terms—Bayesian Reinforcement Learning, Partially Observable Markov Decision Process, Automatic Voltage Control.

NOMENCLATURE

β	Policy Learning Rate
γ	Discount Factor
$\hat{Q}_t(z, z')$	Mean of Posterior distribution $Q(z)$
$\hat{S}_t(z, z')$	Covariance of Posterior distribution $Q(z)$
\mathcal{A}	Action Space
\mathcal{D}_M	Datasets with M rows
\mathcal{O}	Observation Space
\mathcal{S}	State Space
$\nabla_{\theta}\eta(\theta)$	Gradient of expected return
ν	Parameterized Policy
Ω	Observation Probability Distribution
$\phi_{s,s'}^a$	Hyper state
θ	Policy parameters
ξ	Trajectory
$b_t(s)$	Belief State at time t
$G(\theta)$	Fisher Information Matrix
$k(x, x')$	Kernel Functions
k_F	Invariant Fisher Kernel
$KL(p, q)$	Kullback-Liebler Divergence of distribution p & q
M	Number of generators
M_p	Possible actions
N	Number of voltage discretization level
n_b	Number of Buses monitored
n_v	Number of buses with voltage violation
p	Number of action levels
$P_t^{\nu}(z_t)$	t -step State Action occupancy density of policy ν
$Q(s, a)$	State Action Value Function
$R(s, a)$	Reward function
r_p	Residual observation probability

s_t	Current State
s_{t+1}	Next State
t_p	True observation probability
$u(z; \theta)$	Score Function
$V(s)$	State Value Function
$VPI(s, q)$	Value of Perfect Information
z	State-Action pair

I. INTRODUCTION

The increasing complexity of large interconnected power systems makes it difficult to ensure normal grid operation. While automatic controls are deployed to help operators maintain the power grid's reliability and security, a major challenge is how to handle operational uncertainty caused due to cyber intrusions. The cyber defense problem in power systems can hence be framed as a problem of decision making under uncertainty. Reinforcement Learning (RL) with Bayesian inference can help sustain operational reliability under threat.

In an RL problem, an agent interacts with an environment to find an action-selection strategy to optimize its long-term reward. Bayesian Reinforcement Learning (BRL) is a type of RL that uses Bayesian inference to incorporate information into the learning process. It incorporates prior probabilistic distributions and new information, using standard rules of Bayesian inference, and may be model-based or model-free.

The grid's cyber infrastructure enables timely real-time monitoring and actuation of controls. The concern is that challenges such as network congestion, cyber intrusions, and increased misconfigurations may prevent timely and accurate operations. To address this, adversarial RL techniques have been proposed [1], [2], [3], with a cyber intruder modeled as an adversarial agent and a defender agent, as in *CyberBattleSim* [4]. The main contribution of this paper is to present a novel approach to solve the control problem under cyber-induced uncertainty, by detailing a complete framework for modeling a Partially Observable Markov Decision Process (POMDP) based environment for decision-making problems, as the state is not completely observable.

BRL has proven effectual in solving other POMDP problems, e.g., [5], [6]. A Factored Bayes-Adaptive POMDP is proposed in [5] that learns the dynamics of partially observable systems through the Monte-Carlo Tree Search algorithm, while [6] proposes BRL for solving POMDPs with a continuous state space. BRL intrinsically solves the exploration-exploitation problem, as well as incorporates regularization, by avoiding the problem of a few outliers steering it away from true parameters. A frequentist approach of handling parameter uncertainty is computationally infeasible and also requires more

data, since to measure uncertainty, it relies on a null hypothesis and confidence intervals (CI), where $CI = x' \pm z \frac{s}{\sqrt{n}}$ and x' is the sample mean, z is the confidence level value, s is the sample standard deviation and n the sample size. BRL has been utilized in cyber-security management [7], as well as MDPs with model uncertainty [8]. In [7], BRL is introduced for faster intrusion detection, leveraging limited scan results and warnings. For robust adaptation to the real world dynamic environment, a continuous Bayes-Adaptive MDP is proposed [8] and solved using Bayesian Policy Optimization. Unlike the prior works on cyber-security management, this work addresses the voltage control problem in power systems that can encounter cyber-induced data manipulation in the OT network.

The major contributions of this paper are:

- Creation of a cyber-physical POMDP problem for automatic voltage control under uncertainty caused due to FDI attack.
- Propose the use of the BRL techniques to solve the POMDP and Bayesian variants of Deep Q Network (DQN) Learning to improve the performance in comparison to conventional DQN technique.
- Evaluation of the impact of varying prior distribution of the Q function and other parameters of BRL techniques considered for the WSCC and IEEE 14 bus case.

II. BACKGROUND

BRL facilitates the use of explicit probability distributions, which allows uncertainty quantification and enables improved learning strategies. BRL implicitly finds the exploitation/exploration tradeoff and reduces risks in decision making. Exploitation is a greedy approach, where agents try to make the best decision to get more rewards by using an estimated value from the current information. In exploration, agents focus on improving their knowledge about each action to obtain long-term benefits.

In the Bayesian approach, the notion of how certain we are about a state action value function, $Q(s, a)$, is represented through the distribution of $P_Q(s, a)$, which allows us to quantify how much we know about the s, a combination and its reward. A high variance makes the agent explore more, while a low variance provides more certainty; hence, such a combination may not be worth exploring, if a more optimal action is already deciphered by the agent. Moreover, due to its probabilistic framework, one can encode domain knowledge through the prior distribution in BRL. BRL also facilitates regularization by preventing exceptions in the dataset from causing over-fitting problems while learning. Amidst its multiple advantages, the major concern of BRL is that it is computationally expensive, since here we make an estimation of the distribution parameters, unlike point estimates in other RL methods. Utilizing faster algorithms such as [9] that performs High-Dimensional Robust Covariance Estimation can improve the performance but currently is out of scope for discussion in this paper.

Bayesian Stackelberg Markov Games (BSMG) have been leveraged in a proactive Moving Target based Defense (MTD) mechanism for getting rid of an adversary's reconnaissance

stage [10]. Given the adversary competence is unknown, it is inadequate to model the leader-follower games conventionally modeled in MTD problems. Hence, to identify optimal sequential strategies, BSMG are formulated and solved using Bayesian Strong Stackelberg Q-Learning and validated for web-application security in [10].

The automatic voltage control problem has been studied rigorously (e.g., review paper [11]), that use various value and policy learning techniques from RL, but the voltage regulation problems are formulated as an MDP. **This work is the first attempt to formulate the voltage control problem as a POMDP and solve using BRL.**

III. PROBLEM FORMULATION

A. Automatic Voltage Control

Voltage control in power systems is primarily performed through excitation control or voltage regulators at generating stations, through tap changing transformers, induction regulators, shunt reactors and capacitors or synchronous condensers. The automatic voltage control considered in this work is related to the excitation control in which when the terminal voltage drops, the field current is increased to compensate for the voltage drop. A automatic voltage regulator (AVR) detects the terminal voltage and compares it with the reference voltage, with the goal to control the excitation voltage of the generator to cancel out the error (i.e. difference between reference and terminal voltage).

A voltage control problem is formulated, for a three-substation network based on the WSCC 9-bus case [12], with 4 broadcast domains, one for each substation and one for the control center, shown in Fig. 1. The voltages of the 3 generators are regulated, during cyber intrusions targeting FDI attack on the phasor measurements. The control actions are defined as the reference voltage setpoint given to the AVR.

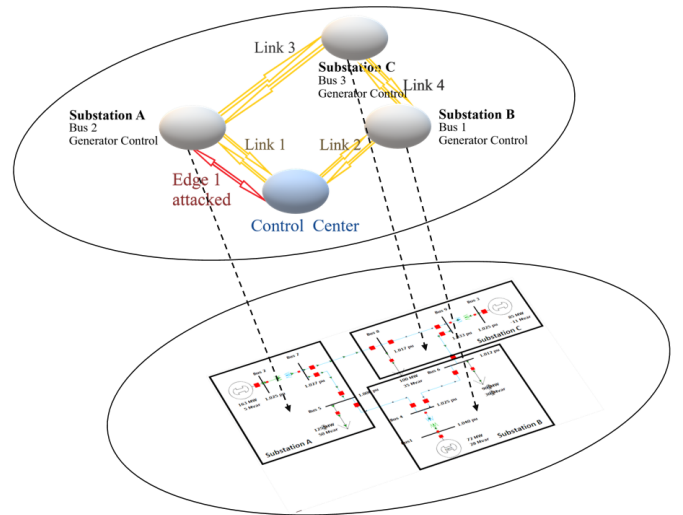


Fig. 1. WSCC 9-Bus Cyber Physical Model

B. Cyber Threat Model

Numerous works on False Data Injection (FDI) attacks and defense exist, such as [13] and [14], on power system state estimation. For FDI attacks, an adversary is considered to be

modifying measurements of devices such as in supervisory control and data acquisition (SCADA) or phasor measurement units (PMUs), to change readings to target the miscontrol of power, based on specific targets. A previous work incorporated FDI in an emulated environment with DNP3 and defense using machine learning [15] [16]. Unlike the previous works on detection, this work aims to control the voltage under cyber threats, through a data-driven RL approach. Hence, this work follows a unique technique of incorporating the FDI through defining an *observation model* in the POMDP space, where the control RL agent observes a different value from the actual state, following a probability distribution. The observation model in the POMDP, $\Omega(o|s)$, is introduced in Section III-F.

C. MDP model

The proposed automatic voltage control under cyber adversarial presence is based on a Markov Decision Process (MDP). A MDP is a discrete-time stochastic process used to describe the agent and environment interactions. In our problem, the agents are compared to the decision making engines, and the environment is the current state of the cyber-physical system, defined by a tuple of five components: states (S), actions (A), state transition model $P(s_{t+1}|s_t, a_t)$ for action a in state s , reward model $R(s_{t+1}|s_t, a_t)$ an agent receives after execution, and discount factor γ that controls future rewards.

The value function $V(s)$ is the benefit for the agent to be in state s , or the expected total reward for an agent starting from state s ; it depends on the policy π used to pick actions. The state-action pair function called the Q-function is also considered. The optimal Q-function $Q^*(s, a)$ is an indication of how good it is for an agent to pick action a while in state s , equal to the summation of immediate reward after performing action a while in state s and the discounted expected future reward after the transition to a next state s' :

$$Q^*(s, a) = R(s, a) + \gamma \sum_{s' \in \mathcal{S}} p(s'|s, a) V^*(s') \quad (1)$$

Next, we describe modifications to this model to account for cyber induced uncertainty by modeling POMDPs. The POMDP can be modeled using notions of both *belief states* and *hyper states* [17]. In the upcoming section, both variants are introduced.

D. Bayes-Adaptive MDP model

The BAMDP [18] is an extension of the MDP and also considered to be a special case of POMDP [17]. The state space of the BAMDP combines jointly the initial set of states S , with the posterior parameters on the transition function Φ , defined collectively as the *hyper-state*.

The Bellman equation for the BAMDP is the following:

$$V^*(s, \phi) = \max_{a \in \mathcal{A}} \left[R(s, a) + \gamma \sum_{s' \in \mathcal{S}} \frac{\phi_{s, s'}^a}{\sum_{s'' \in \mathcal{S}} \phi_{s, s''}^a} V^*(s', \phi') \right] \quad (2)$$

The BAMDP is solved using Bayesian Q-Learning (BQL) (Section IV-A). For the AVC problem, we have discretized the voltage levels from 0.9 to 1.1 p.u. into N levels, because the number of $Q(s, a)$ distributions to be learned needs to be finite. The action space is also discretized for M generators

in the system, with p levels in the range of 0.95-1.05 p.u., resulting in M^p possible actions. Hence the number of Q distributions to learn is $M^p \times N^{n_b}$, where n_b is the number of buses monitored. The reward model for the BAMDP is as follows,

$$R = 50 - 100 * n_v \quad (3)$$

where n_v is the number of buses with violation i.e ($V \geq 1.05$ or $V \leq 0.95$). Assuming $|S|$ states at the start of an episode and a fully-connected state space model, the BAMDP will have $|S|^t$ reachable states at horizon t . Hence, based on t , there is a computational challenge in representing states using *hyper states* [17]. Hence, the belief-state variant of POMDP is considered.

E. POMDP model

In a POMDP [19], the system state is not observable. A POMDP is defined through a tuple $\langle S, A, O, P, \Omega, P_0, R \rangle$, where S is the set of states, A is the set of actions, O is the set of observations, $P(\cdot|s)$ gives the probability distributions over next states, for action a at state s , Ω gives the probability distributions over possible observations, for a at s , P_0 is the probability distribution of initial states, and $R(s, a)$ is a random variable for reward obtained by taking a from s . Since the states are not available, the state space is inferred from the observation and action sequences. This is defined as the information or belief state, updated as follows:

$$b_{t+1}(s') = \frac{\Omega(o_{t+1}|s') \int_S P(s'|s) b_t(s) ds}{\int_S \Omega(o_{t+1}|s'') \int_S P(s''|s) b_t(s) ds ds''} \quad (4)$$

Solving a POMDP obtains an optimal policy ν_* that maximizes the discounted sum of rewards over all information states, through the Bellman equation, where $V^*(b)$ equals:

$$\max_{a \in \mathcal{A}} \left[\int_S R(s, a) b(s) ds + \gamma \int_O \Pr(o|b, a) V^*(\tau(b, a, o)) do \right] \quad (5)$$

and $\tau(b_t, a, o)$ is the b_{t+1} in Eq. 4.

F. POMDP-based AVC Problem

The belief states are updated based on Eq. 4. The observation model for the voltage regulation problem depends on the true observation probability t_p and the residual probability r_p . For example, if a state is 7 (i.e., the voltage value is between 0.96 - 0.97 p.u., for $N = 20$), the probability of observing state 7 will be t_p , while the probability of observing its neighbor states 6 or 8 are $(1 - t_p - r_p)/2$ each, and the probability of observing the rest of the possible states is distributed with r_p . For voltage levels in 0.95 - 1.05 p.u., r_p is kept higher than in the rest of the voltage regions ($r_p(s') \geq r_p(s'')$, where $s' \in (0.95, 1.05)$ and $s'' \geq 1.05 \cup s'' \leq 0.95$). Such formulation keeps the variance of the distribution high for major operating regions.

$$\Omega(o|s) = \begin{cases} t_p & \text{if } o = s \\ 1 - t_p - r_p(s) & \text{if } o \in s - 1, s + 1 \\ r_p(s) & \text{elsewhere} \end{cases}$$

Based on number of voltages monitored n_b , the observation and state space increase exponentially as N^{n_b} . In the results, we analyze the computation complexity of the BRL agents when the state-space increases. The prior of the transition model follows a Dirichlet distribution, as described [20].

Then, based on the discussions and notations above, the reward model for the POMDP is the following,

$$R(s) = 1 - P(\cdot|s) + P(\cdot|s) * R_{orig}(s) \quad (6)$$

where R_{orig} is the actual reward obtained based on Eq. 3.

IV. SOLUTION OF PROPOSED FORMULATION

For solving the models in Sec. III, techniques from Bayesian Reinforcement Learning are considered. An RL algorithm may be model-based or model-free; it may be based on value function, policy search, or a mixed-model approach. Model-based RL explicitly learns the system model (transition probabilities, reward model) and solves the MDP, while model-free RL uses sample trajectories through interaction with the environment. Some RL algorithms learn the value function, such as value iteration, Q-learning, and SARSA [21]. Policy search solves the MDP by direct exploration of the policy, which can grow exponentially with state space size. Hence, policy gradient methods help by defining a differentiable function of a parameterized vector, and the policy is searched as directed by the gradient. Mixed-model techniques include Actor-Critic [22] that uses policy gradient followed by evaluating the policy, estimating a value function.

In BRL, model-based techniques include Bayesian Dynamic Programming, Value of Perfect Information (VPI), and tree-search Q function approximation methods (Bayesian Sparse Sampling, Branch-and Bound Search). Model-free includes Bayesian Deep Q-Network Learning (BDQN), Gaussian Process Temporal Differencing (GPTD), Bayesian Policy Gradient based, and Bayesian Actor-Critic (BAC) (Fig 1.1 of [17]). To solve the proposed problem, we adopt VPI-based Q-learning (model-based), and BDQN and BAC (model-free).

A. Bayesian Q-Learning [23]

In Bayesian Q-Learning, instead of solving for the value function using Eq. 2 for BAMDP, a Dirichlet distribution is used to obtain the state-action values $Q^*(s, a)$ to select the action with highest expected return and value of perfect information (VPI) [23] ($E[q_{s,a}] + VPI(s, a)$). This estimates expected improvement in policy by myopically looking over a single step horizon, following an exploration action. VPI is given as follows:

$$VPI(s, a) = \int_{-\infty}^{\infty} \text{Gain}_{s,a}(x) \text{Pr}(q_{s,a} = x) dx \quad (7)$$

$$\text{Gain}(Q_{s,a}^*) = \begin{cases} E[q_{s,a_2}] - q_{s,a}^* & \text{if } a = a_1 \text{ } q_{s,a}^* < E[q_{s,a_2}] \\ q_{s,a}^* - E[q_{s,a_1}] & \text{if } a \neq a_1 \text{ } q_{s,a}^* > E[q_{s,a_2}] \\ 0 & \text{otherwise} \end{cases} \quad (8)$$

The number of posterior distributions learned is $2 \times N_a \times N_s$, where 2 is due to estimating mean and variance, and N_a and

N_s are the numbers of actions and states, respectively. For the prior, we initialize a random distribution for the mean and variance of the Q. The *PyMC3* library is used for training the model. After the prior is taken in the model, the likelihood is computed based on the observation of Q values from the environment. A Gaussian likelihood is considered. *Variational Inference* [24] with the Adam optimizer is used for obtaining the posterior. The automatic differentiation variational inference works on the principal of finding the optimal posterior distribution q^* , given by the following,

$$q^* = \underset{q \in Q}{\text{argmin}} f(q(\cdot), p(\cdot | y)) \quad (9)$$

where f is the distance between q and p distributions. In variational inference theory, f is the Kullback-Liebler Divergence (KL-Div), where y is the observations/data, and θ is the parameter to be estimated:

$$\begin{aligned} \text{KL}(q(\cdot) \| p(\cdot | y)) &\longrightarrow \int q(\theta) \log \frac{q(\theta)}{p(\theta | y)} d\theta \\ &= \int q(\theta) \log \frac{q(\theta)p(y)}{p(\theta, y)} d\theta = \log p(y) - \int q(\theta) \log \frac{p(\theta, y)}{q(\theta)} d\theta \end{aligned} \quad (10)$$

$KL \geq 0$, and the second expression of the lower-right term in Eq. 10 is the evidence lower bound (ELBO). Eq. 9 is equivalent to maximizing the ELBO. Variational inference works well for Gaussian distributions. For estimating multi-modal distributions, one must consider more advanced techniques such as Stein-Variation Gradient Descent [25] which generates an approximation based on a large number of particles.

B. Bayesian Deep Q Network Learning (BDQN)

The pseudo code for both DQN and BDQN is given in Alg. 1. BDQN combines both MCMC Sampling with the DQN, where the posterior sampling is carried out over the model parameters of the Q network. This is the implementation of the proposed BDQN framework from [26]. In a conventional neural network, weights and biases are found that minimize the error function using gradient-descent optimization called backpropagation with some penalty terms to the loss function for regularization i.e. to prevent overfitting. In the Bayesian approach, instead of training the weights by backpropagation, the weights are proposed based on sampling from Gaussian distribution a proposed weight and evaluating the likelihood $LL(w_p)$ and prior $PL(w_p)$ based on the output of Q network with proposed weight w_p ; further utilizing the Metropolis-Hastings algorithm of computing the acceptance ratio (r), based on which performing the soft update on the target network parameter as performed in DQN. The acceptance ratio, r , is the ratio of the likelihood and prior probability as shown in Line 24 of the Alg. 1, the pseudo code for both DQN and BDQN. In the algorithm, the Line 20-27 is pertaining to the BDQN, while in DQN, Line 16-17 are executed, and the rest of the code is common to both the algorithms.

C. Bayesian Policy Gradient & Actor-Critic Agent

In RL, the policy gradient methods design a parameterized policy and update the parameter through the performance gradient estimate. REINFORCE [21] was the first Monte-Carlo

Algorithm 1 Pseudo Code for BDQN

```

1: function  $BDQN(D, DQN, BDQN)$ 
2:   Initialize  $Q_\theta$  and Target  $Q_{\theta'}$  Network
3:   for each iteration do
4:     for each environment step do
5:       Act  $a_t$  through  $\epsilon$ -greedy
6:       Get  $r_t, s_{t+1}$ 
7:       Store  $(s_t, a_t, r_t, s_{t+1})$  in  $D$ 
8:     end for
9:     for each update step do
10:      Initialize  $w$ , weight of the  $Q$  network
11:      Compute  $LL(w)$  and  $PL(w)$ 
12:      sample  $e_t = (s_t, a_t, r_t, s_{t+1})$  from  $D$ 
13:      Compute target  $Q$  value
14:       $Q^*(s_t, a_t) = r_t + \gamma * Q_{\theta'}(s_{t+1}, \text{argmax}_{a'} Q_{\theta'}(s_{t+1}, a'))$ 
15:      if DQN then
16:        Gradient descent  $(Q^*(s_t, a_t) - Q_\theta(s_t, a_t))^2$ 
17:        Update target N/W  $\theta' = \tau * \theta + (1 - \tau) * \theta'$ 
18:      end if
19:      if BDQN then
20:        for given sample length do
21:           $w_p$  sample a weight from  $N(0, \sigma)$ 
22:           $\tau_p$  sample a  $\tau$  from  $N(0, \sigma)$ 
23:          Compute  $LL(w_p)$  and  $PL(w_p)$ 
24:          Acceptance Ratio  $r = \frac{\min(0, (LL(w_p) - LL(w)) + (PL(w_p) - PL(w)))}{\tau_p}$ 
25:          if  $r \geq U(0, 1)$  then Update target
                network:  $\theta' = \tau_p * \theta + (1 - \tau_p) * \theta'$ 
26:          end if
27:        end for
28:      end if
29:    end for
30:  end for
31: end function

```

based policy gradient technique used in the conventional RL approach, but due to its high variance, other techniques such as Actor-Critic, Advantageous Actor Critic, Proximal Policy Optimization, Natural Policy Gradient, etc., techniques are adopted. In this section, we will explore the Bayesian variant of the above policy gradient techniques which is based on modeling the policy gradient as a Gaussian Process which requires fewer samples to obtain an accurate gradient estimate. A Gaussian process (GP) is an indexed set of jointly Gaussian random variables. The Bayesian Policy Gradient technique considers the complete trajectories as the basic observable unit, hence it cannot take advantage of the Markov property (memoryless stochastic process) when the system is Markovian. In contrast, the BAC (Bayesian Actor Critic) method utilizes the Markov property and leverages Gaussian Process Temporal Differencing (GPTD).

A GP prior is considered for action-value function, $Q(s, a)$, using a prior covariance kernel, then a GP posterior is computed sequentially on every single observed transition. GPTD is a learning model based on a generative model relating the observed reward to the unobserved action-value function given

by:

$$r(z_i) = Q(z_i) - \gamma Q(z_{i+1}) + N(z_i, z_{i+1}) \quad (11)$$

The Fisher kernel is considered as the prior covariance kernel for the GPTD state-action advantage function. For computing the gradient of the policy, the concept of Bayesian Quadrature is utilized, which we will explain in detail further.

The BAC algorithm is an extension of the Bayesian Policy Gradient (BPG) algorithm for learning policies of a continuous state space MDP problem, where the policy is updated by computing the gradient of the expected return given by:

$$\nabla_{\theta} \eta(\theta) = \int \rho(\xi) \frac{\nabla \Pr(\xi; \theta)}{\Pr(\xi; \theta)} \Pr(\xi; \theta) d\xi \quad (12)$$

In the equation, the quantity $\frac{\nabla \Pr(\xi; \theta)}{\Pr(\xi; \theta)}$ is called the Fisher score function. Since the initial state probability distribution P_0 and the state transition probability P are independent of the policy parameter θ The example Gaussian policy distribution with parameter θ is given in the Section V-C. Evaluation of Bayesian Actor Critic Method, for a specific trajectory ξ , we can represent the Fisher score as:

$$u(\xi; \theta) = \frac{\nabla \Pr(\xi; \theta)}{\Pr(\xi; \theta)} = \sum_{t=0}^{T-1} \nabla \log \mu(a_t | x_t; \theta) \quad (13)$$

The Monte Carlo method would utilize a number, say M , of sample paths ξ_i and estimate the gradient $\nabla_{\theta} \eta(\theta)$ using:

$$\widehat{\nabla} \eta(\theta) = \frac{1}{M} \sum_{i=1}^M R(\xi_i) \sum_{t=0}^{T_i-1} \nabla \log \mu(a_{t,i} | x_{t,i}; \theta) \quad (14)$$

where, T_i is the i^{th} episode length. The complete algorithm of the BAC is given by Alg. 2, while Alg. 3 is the procedure to compute the gradient. The variables k_x and k_F introduced in the Alg. 3 are the state kernel and Fisher information kernel. The α and C are the variables associated with the posterior Q computed in the BAC method (refer to [17] for the detailed description):

V. EXPERIMENTAL RESULTS

In the AVC problem, the state space is represented by the bus voltages, while the action space is represented by the set-point of the generators. For the experimentation, two transmission electric grids: a) WSCC and b) IEEE-14 bus case, with 3 and 5 generators respectively are considered. Among the two cases, WSCC case is considered for all the three BRL techniques, while IEEE-14 bus is evaluated for the BDQN technique.

A. Evaluation of Bayesian Q Learning technique

Evaluate various exploration exploitation techniques for Bayesian Q Learning: For the Bayesian Q learning technique, the experiments are performed to keep the voltage at the load buses at the permissible limit. In the WSCC case there are three load buses at Bus 5,6, and 8, among which the average load at Bus 6 is the largest with 185 MW, which is more challenging to regulate the voltage in comparison to bus 5 and

Algorithm 2 Pseudo Code for BAC

```

1: function  $BAC(N_u, N_e)$ 
2:   Initialize  $\theta$ 
3:   for  $i$  in  $N_u$  do
4:     Initialize Fisher Information Matrix,  $G$ 
5:     if  $i \% u_{freq} == 0$  then
6:       Evaluate policy  $\theta$  for  $e_{eval}$  episodes
7:     end if
8:     for  $e$  in  $N_e$  do
9:        $s = env.reset()$ 
10:       $u = Fisher\_Score(s, \theta)$  as per Eq. 13
11:      Till end of episode update  $G = G + u * u'$ 
12:      store  $s, u$  in  $Episodes$ 
13:    end for
14:    Compute  $\Delta\theta = Gradient(Episodes, G)$ 
15:     $\theta = \theta + \beta * \Delta\theta$ 
16:  end for
17: end function

```

Algorithm 3 Pseudo Code for BAC Gradient

```

1: function  $Gradient(Episodes, G)$ 
2:   for  $e$  in  $Episodes$  do
3:     Compute  $G^{-1}$ 
4:     Fisher Info. Kernel  $k_F = u'G^{-1}u \triangleright u$  from  $e$ 
5:     State kernel  $k_x$  is computed using Gaussian func
6:      $k = k_x + k_F$ 
7:     Update  $\alpha, C$  from the episode  $e$  (Eq. ??)
8:   end for
9:   Posterior mean and variance of  $\delta\theta$  is computed to be
    $U * \alpha$  and  $G - U * C * U'$ , where  $U$  is the Fisher score
   vector
10: end function

```

8 with the average of 150 and 100 MW respectively. Three different techniques of exploration-exploitation are considered:

- 1) *Q-Value Sampling*: This sampling technique is based on [27], where the actions are selected stochastically based on the current subjective belief of the action being optimal, i.e., the probability by which an action a is performed is given by

$$\Pr(a = \arg \max_{a'} \mu_{s,a'}) = \Pr(\forall a' \neq a, \mu_{s,a} > \mu_{s,a'}) \quad (15)$$

where the $\mu_{s,a}$ is the mean estimate of the posterior distribution of $Q(s, a)$

- 2) *Greedy selection*: In this technique, the action a that has the highest mean estimate for $Q(s, a)$ for state s is selected.
- 3) *VPI*: It selects the action with highest expected return and VPI i.e. $E[Q_{s,a}] + VPI(s, a)$ as described in Eq. 7.

Fig. 2, Fig. 3, and Fig. 4 show the distribution of the posterior Q value mean obtained with Q-value sampling, greedy, and VPI based techniques, respectively, obtained after completion of certain episodes. Fig. 5 refers to the comparison of these techniques with respect to the average of the episode length to reach the goal state. Both *Q-Value Sampling* and *VPI* techniques perform better in terms of exploration, but Q-

value sampling results in more variance. Based on the average episode length evaluation, the Q-value sampling technique does not result in reduction of episode length unlike the greedy selection and VPI techniques. Hence, based on the Q-value mean distribution as well as the average episode length, we preferred to use the VPI technique in further experiment on selection of better prior Q value distribution.

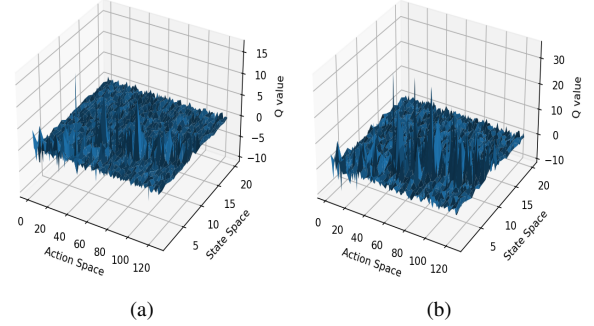


Fig. 2. Evolution of Q value distribution by opting for *Q-Value Sampling* after (a) 1000 episodes (b) 4000 episodes. As more data samples are collected with more number of episodes, the Q values magnitude increases across the diagonal in the State-Action space plane. As the bus-voltage values goes down, the *AVC* agent tries to reduce the set-point due to the ill-formed prior.

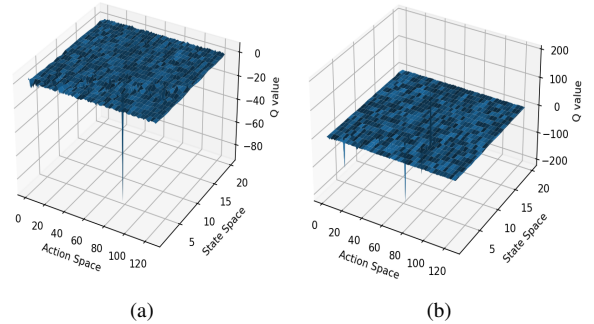


Fig. 3. Evolution of Q value distribution by opting for *Greedy Selection* approach after (a) 1000 episodes (b) 4000 episodes. As more data samples are collected, with more number of episodes, the Q values magnitude in both positive and negative direction increases, hence may not be considered a good option for learning Q values.

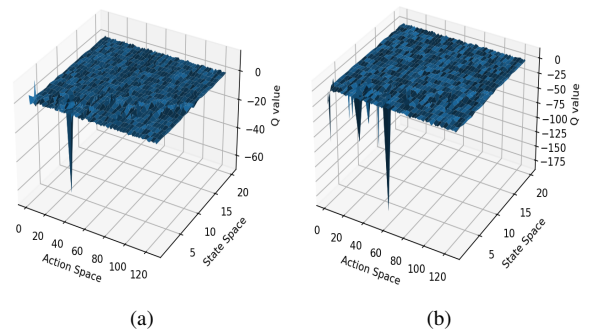


Fig. 4. Evolution of Q value distribution by opting for Q value + *VPI* technique after (a) 1000 episodes (c) 4000 episodes. The performance of the Q value + *VPI* technique is not as good in comparison to Q value sampling technique but it has lesser variance.

Evaluate the effect of selection of good prior for Bayesian Q Learning: Further, we evaluate how a good prior Q

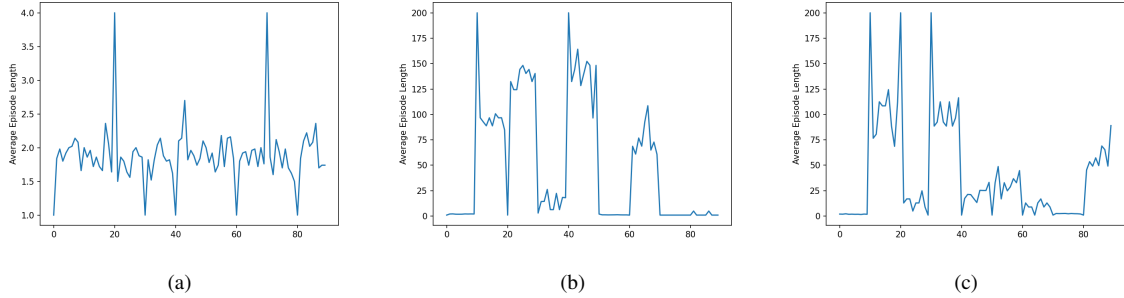


Fig. 5. Comparison of the average episode length for (a) Q value Sampling (b) Greedy Selection (c) Q Val + VPI. The X axis refers to every 50^{th} episode index and Y axis refer to the averaging over 50 episode.

distribution can result in faster convergence in comparison to an ill-formed prior. The ill-formed prior refers to the function, where the actions would favor to lower the voltage set-point when the voltages are already low and to raise the voltage set-point when the voltages are already high; these are given higher Q values in the Q value prior distribution. By contrast, a “good” prior is exactly opposite of the ill-formed prior. Fig. 6 and Fig. 7 show the distribution of the posterior Q value mean using VPI method, after completion of certain episodes. While Fig. 8 refers to the comparison of prior with respect to the average of the episode length to reach the goal state. Similar observations were made on the training and validation average rewards, as shown in Fig. 9. Hence, selection of a better prior distribution can improve the performance as well as result in faster convergence in training the agent in very few episodes.

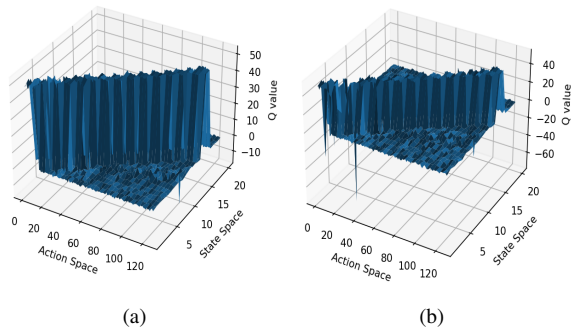


Fig. 6. Evolution of Q value distribution by opting for Q value + VPI technique but with an ill-formed prior after (a) 1000 episodes (b) 4000 episodes. The Q values magnitude are high across the diagonal in the State-Action space plane. As the bus-voltage values goes down, the *AVC* agent reduces the set-point due to the ill-formed prior.

B. Comparison of DQN with Bayesian DQN technique

This section emphasizes on the results on how integration of BDQN agent (introduced in Section IV-B) in comparison to DQN agent assist in training the agent utilizing less trajectories for voltage control. For the WSCC case, with 3 generators and 125 possible actions, Fig. 10 shows how BDQN agent reached the desired goal of having an average reward of 200 in 420 steps while the DQN agent takes more than 580 steps, moreover the reward has higher variance in the DQN case. For the IEEE 14 bus case with 5 generators and 3125 possible actions too the BDQN reaches the goal of average reward of

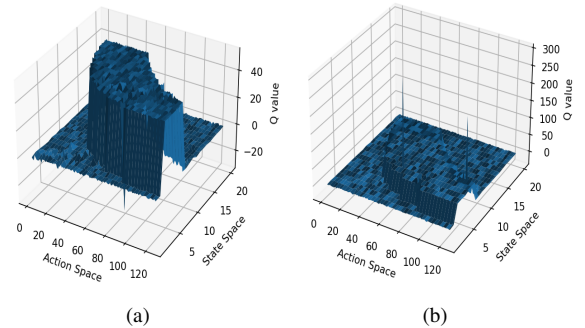


Fig. 7. Evolution of Q value distribution by opting for Q value + VPI technique but with a good prior after (a) 1000 episodes (b) 4000 episodes. The Q values magnitude are high across the cross-diagonal in the State-Action space plane. As the bus-voltage values goes down, the *AVC* agent increases the set-point due to the good prior.

200 in less number of episodes in comparison to the DQN (Figs. 11(a) and 11(b)) for the update frequency uf of 100, 200 and 500, except for the scenario of $uf = 300, 400$ in the BDQN case the average reward had higher variance. Unlike the WSCC case, in the IEEE 14 bus scenario, the network topology were altered in different scenarios, that is one of the probable reason for higher variance in the rewards.

We also evaluate the effect of changing the number of samples considered in the Metropolis Hasting Algorithms used in the MCMC method in BDQN learning. Fig. 12 shows how taking larger samples assist in reaching the goal in less number of training episodes. Similarly update frequency also effects the agent’s training efficiency as shown in Table. V-B

TABLE I Minimum number of episodes to train a BDQN agent with varying update frequency

Update Frequency	Episodes to reach goal
100	111
200	140
300	172
400	168
500	197

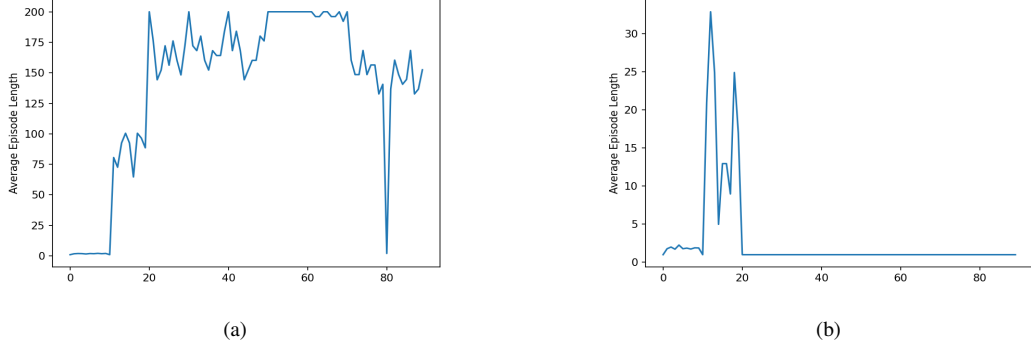


Fig. 8. Comparison of the average episode length for (a) Ill-formed Prior (b) Good Prior. The X axis refers to every 50^{th} episode index and Y axis refer to the averaging over 50 episode.

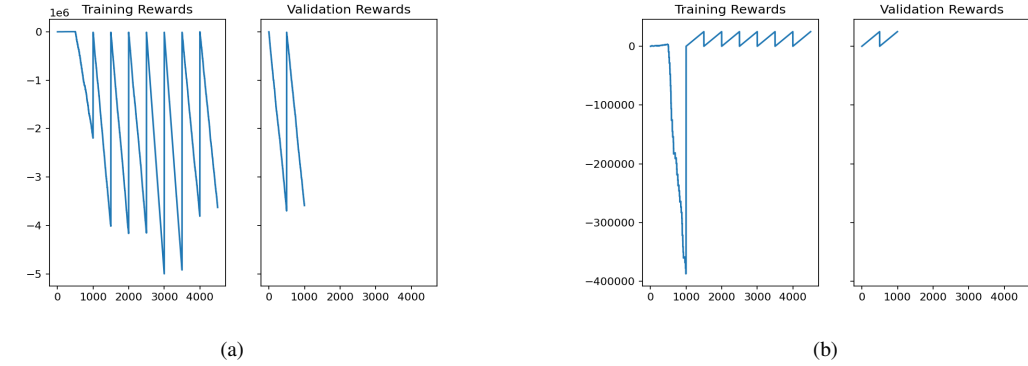


Fig. 9. Comparison of the average training and validation reward for (a) Ill-formed Prior (b) Good Prior. The X axis refers to the episode index.

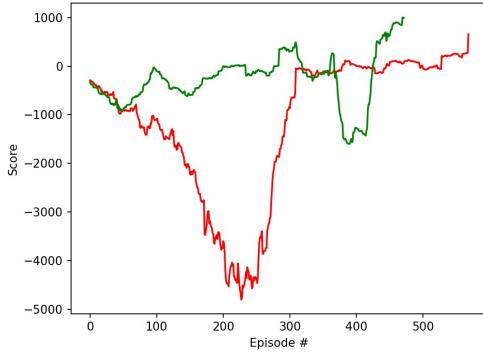


Fig. 10. Comparison of BDQN (in green) and DQN (in red) agents with update frequency of 500 and 50000 samples used in MCMC based BDQN. The score refer to the reward obtained in an episode while training.

C. Evaluation of Bayesian Actor Critic method

In this section, we evaluate the performance of the BAC method on the voltage control problem by taking a certain type of policy function and state space kernel. For the experiments, the policy used has the following form:

$$\mu(a_i | x) = \frac{\exp(\phi(x, a_i)^\top \theta)}{\sum_{j=1}^{125} \exp(\phi(x, a_j)^\top \theta)}, \quad i = 1, 2, \dots, 125 \quad (16)$$

where, 125 are the possible actions since there are 3 generators for the WSCC case with 5 discrete voltage levels of set-points. The policy feature vector $\phi(x, a_i) = (\phi(x)^\top \delta_{a_1, a_i}, \dots, \phi(x)^\top \delta_{a_{125}, a_i})$, where δ_{a_j, a_i} is 1, if $a_j = a_i$ and 0 otherwise. While the state feature vector/ Gaussian State Kernel $\phi(x)$ is represented as follows:

$$\phi(x) = (\exp(-\frac{\|x - \bar{x}_1\|^2}{2\sigma^2}), \dots, \exp(-\frac{\|x - \bar{x}_L\|^2}{2\sigma^2})) \quad (17)$$

where, L is the number of voltage levels the state is discretized and σ^2 refers to the variance of the Gaussian function. The x is the p.u. voltage while the x_1 refers to the center of the first level in the voltage space and x_L being the center of the last level. After every u_{freq} (policy update frequency), the learned policy is evaluated for $e_{eval} = 10$ episodes to estimate accurately the average number of steps to goal as well as the average episodic reward. We evaluate the performance by varying the voltage levels as well exploring the option with using different number of generators, to observe the effect of varying action space. The selection of variance σ^2 can also effect the result, but currently this is not considered for evaluation. The BAC learning parameters are shown in Table II.

Evaluation of the voltage discretization level: With increase in voltage levels, the state space increases so as the number of terms in the Gaussian State Kernel, which may cause more episodes for the policy to converge hence it can be observed from the Fig. 13, the average number of episodes is less in

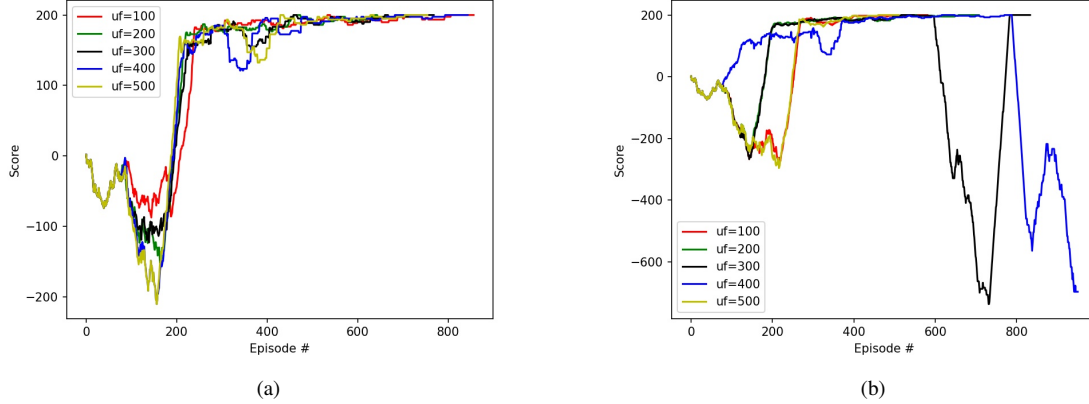


Fig. 11. Evaluation of the effect of the policy update frequency (uf) for IEEE 14 bus systems using (a) DQN (b) BDQN. Lower the uf value faster the target score of 200 is reached in BDQN. During the training, BDQN agent reaches the target goal score in less episodes in comparison to DQN.

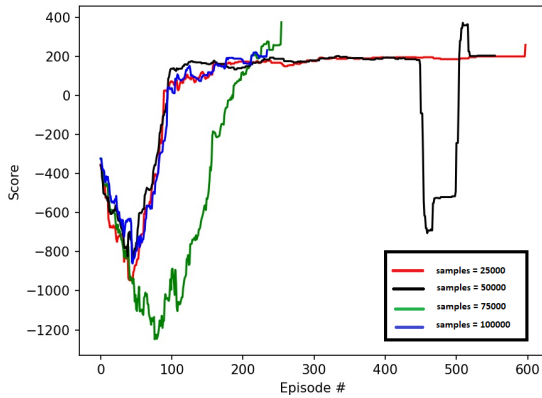


Fig. 12. Evaluation of number of samples on the BDQN agent average reward with a fixed update frequency of 500 episodes.

TABLE II BAC Learning parameters

Param	Desc	Val
N_u	Max. # of policy updates	200
u_{freq}	# of policy updates per evaluation	[5-25]
N_e	# of episodes for every policy update	10
e_{eval}	# of episodes in each evaluation	10
β	Gradient Learning Rate	[.0025]
e_{max}	Each episode maximum length	10
γ	Discount Factor	0.99
L	Voltage Discretization Level	[10,20]

the case of $L = 10$ in comparison to $L = 20$, but there is a decreasing trend in the case of $L = 20$, which have better accuracy and less variance while proceeding towards obtaining optimal policy. Even the average episodic rewards have a more increasing trend with the scenario of $L = 20$. Higher the levels the policy gradient technique can become computationally more expensive, but based on the improvement of performance $L = 20$ is considered further to evaluate the effect of learning rate β and update frequency u_{freq} in the subsequent sub-

section. The dotted lines in the figures, show the polynomial trendline.

Effect of BAC Learning Rate: The amount of change to the BAC model during each step, is the learning rate, β , and is one of the most important hyper-parameter for training. It determines how quickly or slowly the model learns. Higher learning rate generally allows the model to learn faster but results in sub-optimal policies. Fig. 14 shows the effect of the learning rate β on the mean square error (based on the deviation of the bus voltage values from 1.0 p.u.), average episode length and average episodic reward. Among three different β values, $\beta = .0025$ is better and $\beta = .005$ is worse among all. Hence, we further consider $\beta = .0025$ for the experiments to study the effect of u_{freq} of the BAC algorithm. The dotted lines in the figures, show the polynomial trendline.

Effect of BAC policy update frequency: Line 5 in the Algorithm 2 shows the frequency with which we evaluate the trained policy parameter θ . Fig. 15 shows the effect of the update frequency, u_{freq} , on the mean square error, average episode length and average episodic reward. The $u_{freq} = 15, 25$ performs better with non-negative rewards and low average episode length, quite early in the validation index. Usually it is suggested to update with enough transitions captured through the episodes before doing a policy updates, but that would again depend on other factors such as how difficult the environment were. The results for the Bayesian Actor Critic (BAC) method can be further improved by considering other kernel functions and exploring more hyper-parameters.

VI. CONCLUSION

In this work, a POMDP for automatic voltage regulation in the transmission grid is formulated and solved using various BRL techniques. The major findings were: **a)** BDQN outperforms DQN agents in training the agents in less number of episodes. **b)** Value of Perfect Information based exploration-exploitation techniques improved the performance of the Bayesian-Q learning technique. **c)** Selection of an appropriate prior Q distribution plays a major role in the Bayesian Q learning process. **d)** Bayesian Actor Critic method is evaluated

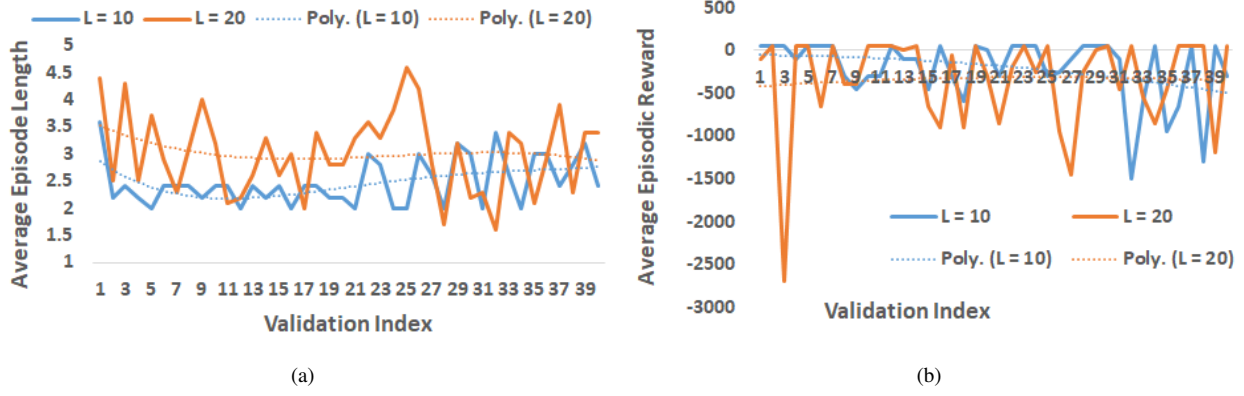


Fig. 13. Comparison of (a) Average Episode Length (b) Average Episodic Reward for two different voltage discretization levels $L = 10$ and $L = 20$

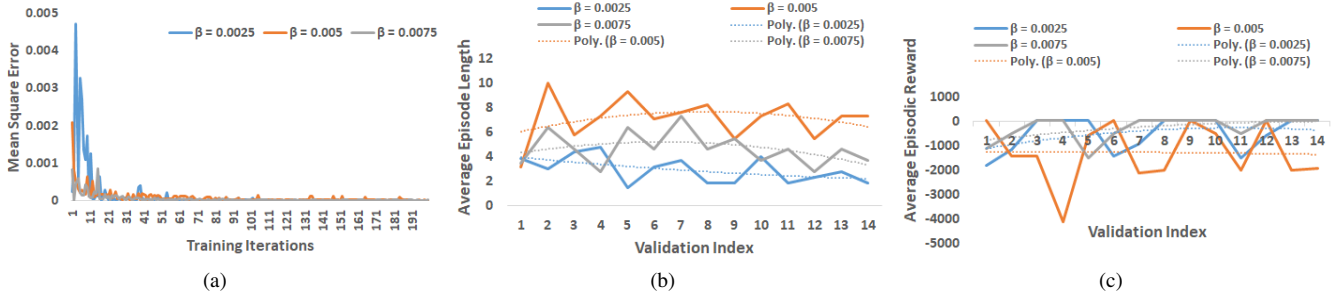


Fig. 14. Effect of varying learning rate, β , of the BAC policy gradient algorithm based of (a) Mean Square Error (b) Average Episode Length (c) Average Episodic Reward

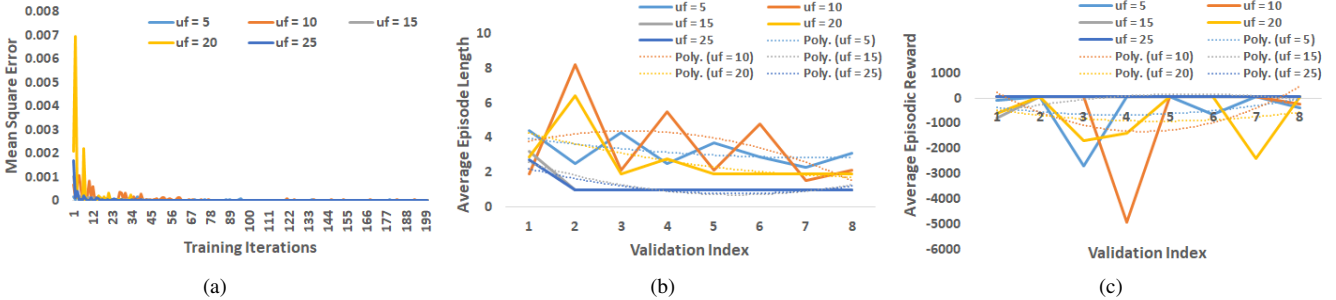


Fig. 15. Effect of varying update frequency u_{freq} of the BAC policy gradient algorithm based of (a) Mean Square Error (b) Average Episode Length (c) Average Episodic Reward

on the basis of the impact of hyper-parameters on the learning performance.

ACKNOWLEDGEMENT

This work is supported by funds from the US Department of Energy under award DE-OE0000895.

REFERENCES

- [1] S. Paul, Z. Ni, and C. Mu, "A learning-based solution for an adversarial repeated game in cyber-physical power systems," *IEEE Transactions on Neural Networks and Learning Systems*, vol. 31, no. 11, 2020.
- [2] A. Pan, Y. Lee, H. Zhang, Y. Chen, and Y. Shi, "Improving robustness of reinforcement learning for power system control with adversarial training," 2021. [Online]. Available: <https://arxiv.org/abs/2110.08956>
- [3] L. Omnes, A. Marot, and B. Donnot, "Adversarial training for a continuous robustness control problem in power systems," 2020. [Online]. Available: <https://arxiv.org/abs/2012.11390>
- [4] C. Seifert, J. Bono, J. Parikh, and W. Blum, "Cyberbattlesim," Microsoft, Feb 2020. [Online]. Available: <https://www.microsoft.com/en-us/research/project/cyberbattlesim/>
- [5] S. Katt, F. A. Oliehoek, and C. Amato, "Bayesian reinforcement learning in factored pomdps," in *Proceedings of the 18th International Conference on Autonomous Agents and MultiAgent Systems*, ser. AAMAS '19. Richland, SC: International Foundation for Autonomous Agents and Multiagent Systems, 2019, p. 7.
- [6] P. Dallaire, C. Besse, S. Ross, and B. Chaib-draa, "Bayesian reinforcement learning in continuous pomdps with gaussian processes," 12 2009, pp. 2604–2609.
- [7] T. Allen, S. Roychowdhury, and E. Liu, "Reward-based monte carlo-bayesian reinforcement learning for cyber preventive maintenance," pp. 578–594, 2018. [Online]. Available: <https://www.sciencedirect.com/science/article/pii/S0360835218304674>
- [8] G. Lee, B. Hou, A. Mandalika, J. Lee, S. Choudhury, and S. S. Srinivasa, "Bayesian policy optimization for model uncertainty," 2018. [Online]. Available: <https://arxiv.org/abs/1810.01014>
- [9] Y. Cheng, I. Diakonikolas, R. Ge, and D. Woodruff, "Faster algorithms for high-dimensional robust covariance estimation," 2019. [Online].

Available: <https://arxiv.org/abs/1906.04661>

- [10] S. Sengupta and S. Kambhampati, "Multi-agent reinforcement learning in bayesian stackelberg markov games for adaptive moving target defense," *CoRR*, vol. abs/2007.10457, 2020. [Online]. Available: <https://arxiv.org/abs/2007.10457>
- [11] X. Chen, G. Qu, Y. Tang, S. Low, and N. Li, "Reinforcement learning for selective key applications in power systems: Recent advances and future challenges," *IEEE Transactions on Smart Grid*, vol. 13, no. 4, pp. 2935–2958, 2022.
- [12] I. C. for a Smarter Electric Grid (ICSEG), "Wscg 9-bus system." [Online]. Available: <https://icseg.iti.illinois.edu/wscg-9-bus-system/>
- [13] A. Kundu, A. Sahu, E. Serpedin, and K. Davis, "A3d: Attention-based auto-encoder anomaly detector for false data injection attacks," *Electric Power Systems Research*, vol. 189, 2020.
- [14] O. Boyaci, A. Umunnakwe, A. Sahu, M. R. Narimani, M. Ismail, K. R. Davis, and E. Serpedin, "Graph neural networks based detection of stealth false data injection attacks in smart grids," *IEEE Systems Journal*, vol. 16, no. 2, pp. 2946–2957, 2022.
- [15] A. Sahu, P. Wlazlo, Z. Mao, H. Huang, A. Goulart, K. Davis, and S. Zonouz, "Design and evaluation of a cyber-physical testbed for improving attack resilience of power systems," *IET Cyber-Physical Systems: Theory & Applications*, 2021.
- [16] A. Sahu, Z. Mao, P. Wlazlo, H. Huang, K. Davis, A. Goulart, and S. Zonouz, "Multi-source multi-domain data fusion for cyberattack detection in power systems," *IEEE Access*, vol. 9, 2021.
- [17] M. Ghavamzadeh, S. Mannor, J. Pineau, and A. Tamar, "Convex optimization: Algorithms and complexity," *Foundations and Trends® in Machine Learning*, vol. 8, no. 5-6, pp. 359–483, 2015. [Online]. Available: <https://doi.org/10.1561%2F22000000049>
- [18] M. O. Duff and A. G. Barto, "Optimal learning: computational procedures for bayes-adaptive markov decision processes," 2002.
- [19] G. E. Monahan, "A survey of partially observable markov decision processes: Theory, models, and algorithms," vol. 28. Management Science, 1982, pp. 1–16. [Online]. Available: <http://www.jstor.org/stable/2631070>
- [20] M. Strens, "A bayesian framework for reinforcement learning," *Proceedings of the Seventeenth International Conference on Machine Learning*, 02 2001.
- [21] R. S. Sutton and A. G. Barto, *Reinforcement Learning: An Introduction*, 2nd ed. The MIT Press, 2018. [Online]. Available: <http://incompleteideas.net/book/the-book-2nd.html>
- [22] V. Konda and J. Tsitsiklis, "Actor-critic algorithms," in *Advances in Neural Information Processing Systems*, S. Solla, T. Leen, and K. Müller, Eds., vol. 12. MIT Press, 1999. [Online]. Available: <https://proceedings.neurips.cc/paper/1999/file/6449f44a102fde848669bdd9eb6b76fa-Paper.pdf>
- [23] R. Dearden, N. Friedman, and S. Russell, "Bayesian q-learning," ser. AAAI '98/IAAI '98. USA: American Association for Artificial Intelligence, 1998, p. 761–768.
- [24] D. M. Blei, A. Kucukelbir, and J. D. McAuliffe, "Variational inference: A review for statisticians," *Journal of the American Statistical Association*, vol. 112, no. 518, p. 859–877, Apr 2017. [Online]. Available: <http://dx.doi.org/10.1080/01621459.2017.1285773>
- [25] Q. Liu, "Stein variational gradient descent as gradient flow," 2017. [Online]. Available: <https://arxiv.org/abs/1704.07520>
- [26] R. M. Neal, "Bayesian learning for neural networks," *Ph.D. Thesis*, 1997.
- [27] J. Wyatt, "Exploration and inference in learning from reinforcement," *Ph.D. Thesis*, 1997.